Available online at www.sciencedirect.com

SciVerse ScienceDirect

Acta Materialia 60 (2012) 1287–1292

Acta MATERIALIA

www.elsevier.com/locate/actamat

Core structure of a screw dislocation in Ti from density functional theory and classical potentials

M. Ghazisaeidi [a], D.R. Trinkle [b,*]

[a] Department of Mechanical Science and Engineering, University of Illinois at Urbana-Champaign, Urbana, IL 61801, USA
[b] Department of Materials Science and Engineering, University of Illinois at Urbana-Champaign, Urbana, IL 61801, USA

Received 14 September 2011; received in revised form 11 November 2011; accepted 13 November 2011

Abstract

Previous density functional theory (DFT) studies of the 1/3 $\langle 1\bar{2}10\rangle$ screw dislocation in titanium have shown metastable core structures depending on the initial position of the dislocation line. We investigate this problem by modeling a screw dislocation with two initial positions using both DFT and a modified embedded atom (MEAM) potential for Ti with flexible boundary conditions. Both DFT and MEAM produce initial-position-dependent core structures. The MEAM potential stacking fault energies and core structures are in good agreement with DFT. MEAM potential computes the core energies and shows the behavior of both cores under applied strain. We found that the higher-energy core always reconstructs into the lower-energy one independent of the applied strain direction. Transformation from low- to high-energy core was not observed. Therefore, at $T = 0$ K, only the low-energy core is stable under applied strain.

Keywords: Titanium; Dislocations; Plastic deformation; Core structure; Density functional theory

1. Introduction

The core structure and mobility of dislocations directly relate to mechanical properties of materials [1]. Accurate atomic-scale dislocation core geometry is important for high stacking fault materials such as Ti where the dislocation core is compact and therefore difficult to investigate by experiments. Classical potential studies predict both prismatic and basal core spreading for screw dislocations in Ti depending on the origin of the initial elastic displacement field [2,3]. The prismatic core is expected for Ti where slip on the prism planes is dominant. Recently, Tarrat et al. studied the core geometry of the $1/3[1\bar{2}10]$ screw dislocation in Ti within the cluster approach with density functional theory (DFT) [4] and showed that two different metastable core structures are possible depending on the origin for the elastic displacement field of the dislocation imposed before the relaxations. One of the cores is symmetrically prismatic—with the lowest excess energy—while the other shows a combination of prismatic and pyramidal spreading. We consider this problem to identify (a) if the existence of metastable cores is an artifact of the boundary conditions and (b) if the cores can be easily transformed from one to the other (e.g. cross-slip or transition states). We model the isolated dislocation using flexible boundary conditions where the lattice Green's function (LGF) couples the core to the far-field harmonically responding medium, eliminating the spurious effects of free surfaces or insufficient computational cell size in the cluster approach. Flexible boundary conditions have successfully modeled dislocation cores in Mo, Al, Pd and Mg [5–8]. In addition to DFT, we use a modified embedded atom (MEAM) potential for Ti [9] to investigate the dependence of core geometry metastability on the potential and to study the behavior under stress.

Section 2 presents the computational details for flexible boundary conditions with DFT. Comparison between MEAM potential and DFT stacking fault energies (SFEs) shows good agreement in Section 3. Section 4 finds that the metastable cores are not artifacts of the boundary

* Corresponding author.
E-mail addresses: mghazis2@illinois.edu (M. Ghazisaeidi), dtrinkle@illinois. edu (D.R. Trinkle).

1359-6454/$36.00 © 2011 Acta Materialia Inc. Published by Elsevier Ltd. All rights reserved.
doi:10.1016/j.actamat.2011.11.024

conditions or the potential. In addition, as the MEAM potential reproduces the DFT geometry, we can determine the relative energy ordering and the effect of stress. The higher-energy core easily transforms to the lower-energy one with applied stress. We do not observe the transformation to the higher-energy core (i.e. cross-slip) which suggests that modeling the low-energy core is sufficient for studies of plastic deformation.

2. Computational method

Isolated dislocations are modeled using flexible boundary conditions [10,5]. Periodic boundary conditions are applied along the dislocation line. Flexible boundary conditions relax atoms surrounding the dislocation core region with the LGF as if they are embedded in an infinite harmonic crystalline medium. The initial condition for relaxation is the anisotropic elasticity solution for the perfect screw dislocation displacement field applied to all atoms. Flexible boundary conditions divide the simulation geometry into three regions: core (I), transition (II) and buffer (III). Force calculations are done with DFT or MEAM throughout the whole geometry. The conjugate gradient method relaxes the atoms around the core (region I); displacements in region I generate forces on atoms of the transition region (II). The LGF removes the forces on region II by adding corrective displacements to all atoms. The outermost region (III) acts as a buffer to protect forces in regions I and II from the boundaries or free surfaces on the simulation cell. Atoms in the buffer region are only displaced by the corrective displacements of the LGF update stage. Relaxation in region I (conjugate gradient) and region II (LGF update) is iterated until the forces in regions I and II are smaller than a chosen threshold (20 meV/Å here).

DFT calculations are performed with VASP [11,12], a plane-wave-based density functional code using the projected augmented wave method within the generalized gradient approximation [13]. The 4s and 3d electrons in Ti are treated as valence electrons. A planewave energy cut-off of 290 eV ensures energy convergence to 0.05 meV/atom. The k-point mesh consists of 16 k-points along the dislocation line and 1 k-point in each of the orthogonal directions in the plane perpendicular to the threading direction. This k-point mesh with Methfessel–Paxton smearing of 0.2 eV gives an energy accuracy of 0.1 meV/atom for bulk Ti. The screw dislocation supercell has 621 (I:41, II:196, III:384) atoms. We modeled the same screw dislocation in a 882 (I:162, II:286, III:434) atom supercell with MEAM instead of DFT. We used the MEAM calculation to estimate the core spreading and to determine the smallest possible size for DFT calculations (i.e. the limit on region I); hence, the MEAM cell is bigger than the DFT cell.

Fig. 1 shows the simulation cells used in DFT and MEAM calculations. The MEAM supercell is terminated in vacuum. Classical potential relaxations are done using the LAMMPS package [14]. Since we are interested in the solution only in regions I–III, including a vacuum region in DFT calculations is inefficient. Moreover, the electrons can form a charge dipole at the metal surface and create image forces in region III. In the case of screw dislocations, a periodic simulation cell with domain boundaries at the edges of the cell can be used instead. Using domain boundaries leads to smaller charge density perturbations and smaller cell sizes [15].

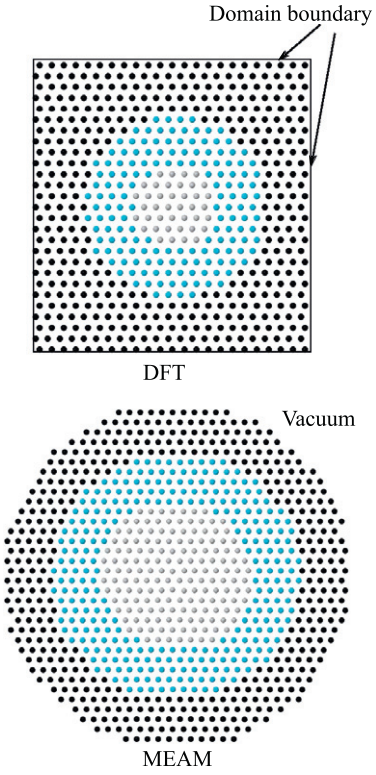

Fig. 1. Simulation cells used in DFT and MEAM calculations. Gray, blue and black correspond to regions I, II and III, respectively. The DFT supercell has domain boundaries at the edges of the periodic cell. The MEAM supercell is surrounded by vacuum and is not repeated in the plane perpendicular to the dislocation line. Both cells are periodic along the dislocation line into the plane of view along $[1\bar{2}10]$.

3. Stacking fault energies

For Ti, a prismatic stacking fault is the lowest in energy and has a geometry that strongly influences the dislocation core structure and mobility. In a hexagonal close-packed (hcp) structure, the $(10\bar{1}0)$ prism planes are separated by a/3 or 2a/3. Therefore, two types of prismatic stacking faults are possible: the "easy" and "hard" stacking faults which are created between a widely spaced or a closely spaced pair of prism planes, respectively; both appear in the dislocation core. Fig. 2 shows the generalized SFE surface for an easy prismatic stacking fault in Ti from DFT and MEAM. The generalized stacking fault surface for the prism plane is defined by displacing a single $(10\bar{1}0)$ prismatic plane by a linear combination of $[0001]$ and $1/3[1\bar{2}10]$. The faulted geometry is allowed to relax in the $[10\bar{1}0]$ direction. Repeating this procedure for various

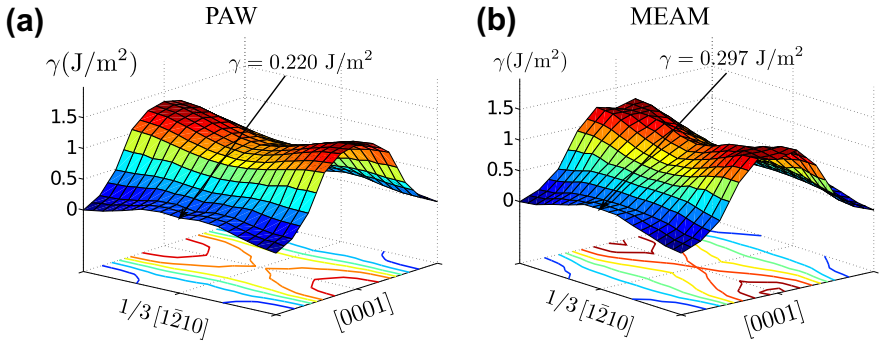

Fig. 2. Generalized stacking-fault energy surface for $(10\bar{1}0)$ prism plane in Ti from: (a) DFT and (b) MEAM. Stacking fault displacements along $[1\bar{2}10]$ appear in the $1/3\langle 1\bar{2}10\rangle$ screw dislocation core. The point corresponding to 50% slip along $[1\bar{2}10]$ direction is a local minimum with $\gamma = 0.220$ J/m^2 in (a) and a saddle point with $\gamma = 0.297$ J/m^2 in (b).

Table 1
Stacking fault energies from DFT and MEAM. Easy and hard prismatic and pyramidal SFEs γ_{easy}, γ_{hard} and γ_{pyram} are evaluated at $1/6[1\bar{2}10]$. γ_{I2} corresponds to the metastable intrinsic stacking fault on the basal plane (0001) at the fault displacement vector $1/3[10\bar{1}0]$.

J/m^2	γ_{easy}	γ_{hard}	γ_{pyram}	γ_{I2}
DFT	0.220	1.185	0.689	0.292
MEAM	0.297	1.495	0.443	0.172

displacement vectors gives the generalized stacking-fault energy or the gamma surface. Our results show that MEAM SFE values generally agree well with those obtained from DFT. Stacking fault displacements along $[1\bar{2}10]$ appear in the $1/3\langle 1\bar{2}10\rangle$ screw dislocation core. Note that $1/6[1\bar{2}10]$ is a local minimum ($\gamma = 0.220$ J/m^2) with DFT and a saddle point ($\gamma = 0.297$ J/m^2) with MEAM. Table 1 compares DFT and MEAM SFEs at representative points. Easy and hard prismatic SFE and pyramidal SFE are evaluated at $1/6[1\bar{2}10]$. DFT and MEAM hard prismatic SFEs are five times higher than the corresponding easy prismatic and pyramidal SFEs. Note that with DFT, basal I2 SFE is higher than the easy prismatic, while with MEAM, basal SFE is the smallest.

Fig. 3a shows the projection of the $(10\bar{1}1)$ pyramidal gamma surface computed by MEAM. The fault displacement vector $\vec{t} = 1/2[\bar{1}012] + 1/6[1\bar{2}10] = 1/3[\bar{1}\bar{1}23]$ corresponds to a lattice vector and consequently gives a zero SFE (white square in Fig. 3a). To compare with DFT, we computed the pyramidal SFE along the $[1\bar{2}10]$ path shown by a white arrow in Fig. 3a. Fig. 3b shows that MEAM pyramidal SFEs are lower than the DFT values.

4. Dislocation core structures

Figs. 4 and 5 show the core structure of the $1/3[1\bar{2}10]$ screw dislocation in Ti obtained from DFT and MEAM at two initial positions for the origin of the elastic solution for a perfect screw dislocation. The red[1] squares indicate the initial centers; while the long-range solution is the same, there can be variations in the relaxed core geometry. Tarrat et al. considered five initial positions and reported the geometry of two different core structures [4]. They compared the DFT core structures to the results from a EAM potential. In one case, both EAM and DFT gave a symmetric prismatic core. The other initial position caused the EAM core to spread on the basal plane while DFT showed a combination of prismatic and pyramidal spreading [4]. What Tarrat et al. called position 3 (a symmetric prismatic core), we refer to as "mirrored", and we refer to their position 5 as "unmirrored" in reference to the mirror plane in (0001).

Figs. 4 and 5 show the core structure of our mirrored and unmirrored cores analyzed with full and partial differential displacement (DD) maps [16] and Nye tensor density [17]. Figs. 4a and b and 5a and b show the full DD maps of the cores. Each circle is a row of atoms along the dislocation threading direction (i.e. out of the plane), where an arrow between two rows of atoms corresponds to the relative displacement between the rows compared with the perfect crystal. The length of the arrow scales as the magnitude of the relative displacement between atom rows. A closed triad of arrows shows a Burger's vector displacement. Our results confirm the existence of metastable core structures depending on the initial position of the dislocation line. In addition, MEAM and DFT core geometries agree very well in each case. Furthermore, we study the structure of the partial dislocations for both cores. Figs. 4 and 5c–h show the Nye tensor distribution superimposed on the DD maps of the dissociated partials for mirrored and unmirrored cores, respectively. Color contours in Figs. 4 and 5 show the linear interpolation of the Nye tensor density following the method of Hartley and Mishin [17]. The Nye tensor's screw component and edge components on basal and prism planes are plotted in each case. Partial dislocations are identified by local extrema in the Nye tensor distribution or a closed triad of atoms in DD maps. In these maps closed triads represent a half Burger's vector to identify the partials. The mirrored core dissociates into two screw character partials separated by less than 2c on the

[1] For interpretation of color in Figs. 1–6, the reader is referred to the web version of this article.

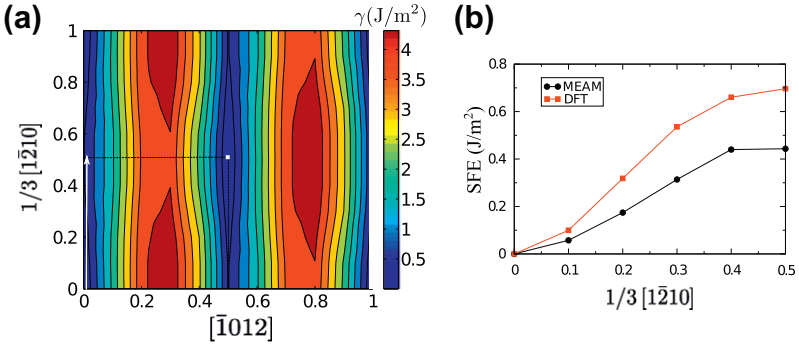

Fig. 3. Projection of the $(10\bar{1}1)$ pyramidal plane generalized SFE for MEAM (a) and its cross-section along the $1/3[1\bar{2}10]$ direction for MEAM and DFT (b). The white square is located at $1/2[\bar{1}012] + 1/6[1\bar{2}10]$, which corresponds to a zero SFE value. (b) Shows the MEAM and DFT values of the SFE in the pyramidal plane along the white arrow.

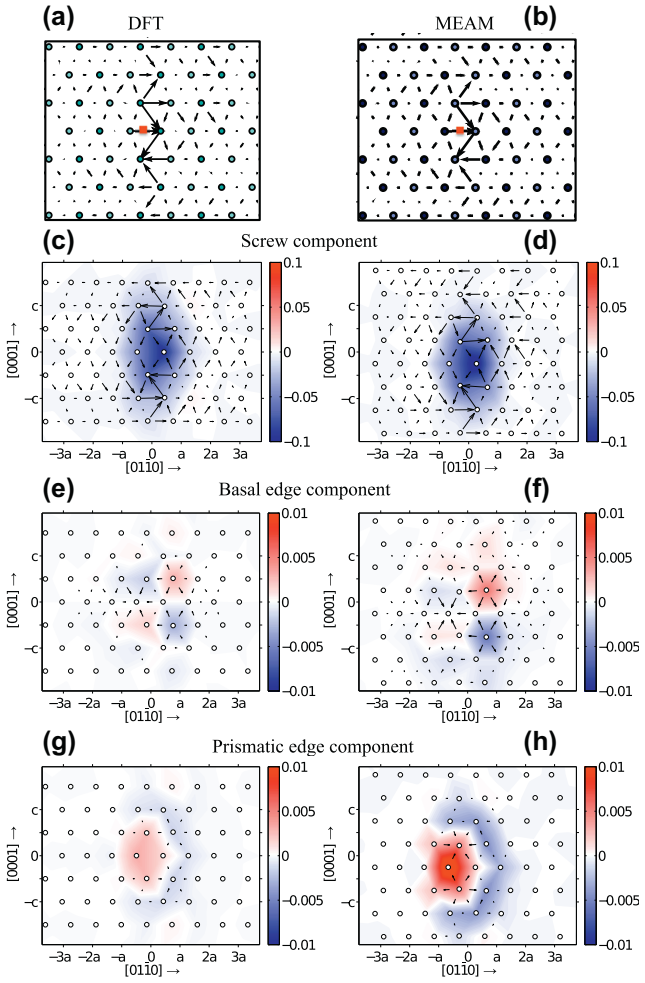

Fig. 4. Mirrored core structure of the dissociated $1/3[1\bar{2}10]$ screw dislocation (the lower-energy core between two metastable configurations). The red square shows the origin of the elastic solution for the perfect dislocation. Contour plots of the screw and edge components of the Nye tensor are plotted. DD maps of the dissociated dislocations are superimposed. Partial dislocations are identified by local extrema in the Nye tensor distribution or a closed triad of atoms in DD maps. The core spreading onto the prism planes is similar between DFT and MEAM. Note the change of scale by an order of magnitude from the screw component to the edge component plots.

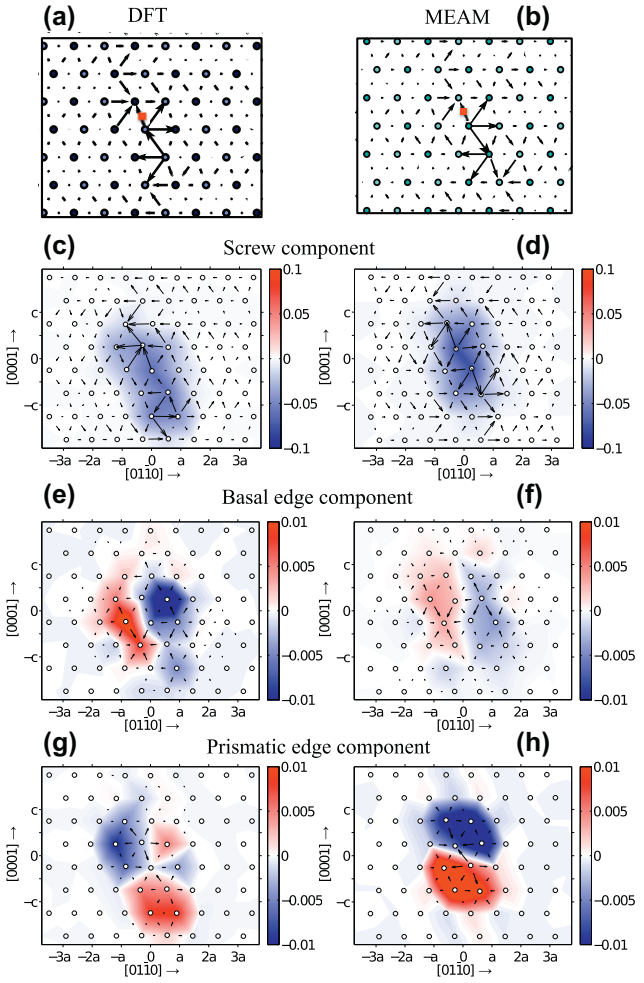

Fig. 5. Unmirrored core structure of the dissociated $1/3[1\bar{2}10]$ screw dislocation (the higher-energy core between two metastable configurations). The red square shows the origin of the elastic solution for the perfect dislocation. Contour plots of the screw and edge components of the Nye tensor are plotted. DD maps of the dissociated dislocations are superimposed. Partial dislocations are identified by local extrema in the Nye tensor distribution or a closed triad of atoms in DD maps. Both DFT and MEAM show similar non-planar core spreading, almost along the pyramidal plane. Note the change of scale by an order of magnitude from the screw component to the edge component plots.

prismatic plane. Both MEAM and DFT give the same compact core with symmetrical prismatic spreading. Unmirrored core partials have both screw and edge character and form a non-planar core structure.

We compute the excess energy between the two cores by subtracting the energies of region I atoms in each core using MEAM. We find that the unmirrored core is about 12 meV/b higher in energy where b is the magnitude of the dislocation's Burger's vector. Note that the initial position of the mirrored core is located between a widely spaced pair of prism planes and exactly on a basal plane. In this case, dislocation displacements tend to create an easy prismatic stacking fault in the core without a possibility of displacing basal planes. The low value of γ_{easy} allows these displacements and creates a symmetric prismatic core. On the other hand, the initial position of the unmirrored core is located between closely spaced prismatic planes and halfway between two basal planes. Here, the dislocation displacement field induces a hard prismatic stacking fault which requires a very high energy according to Table 1. Therefore, a combination of a basal followed by an easy prismatic fault creates the non-planar core.

We investigate the behavior of screw cores under applied strain and find that the mirrored core is stable. Since the prismatic plane is the dominant slip plane for the glide of the screw dislocation, we compute the strain required to move the dislocation by applying strain on the prism planes. In order to find the minimum stress, the dislocation core geometry should be relaxed under several incrementally increasing strain values. These are computationally expensive calculations derived from DFT. On the other hand, the MEAM potential predicts the SFEs and dislocation core geometries very well while being computationally cheap and thus is used to perform strain calculations. Fig. 6 shows the mirrored and unmirrored cores under applied strain on the prism planes. We found that the mirrored core starts to move under $\epsilon_{\text{prism}} = 0.005$ prismatic strain. The higher-energy unmirrored core reconstructs into the lower-energy mirrored core and begins to move on the prismatic plane at $\epsilon_{\text{prism}} = 0.007$. Since the unmirrored core is non-planar, we also put the cores under strain $\epsilon_{\text{pyramidal}}$ on the pyramidal plane for testing purposes. The mirrored core begins to slip on the prism plane under $\epsilon_{\text{pyramidal}} = 0.005$ pyramidal strain. At $\epsilon_{\text{pyramidal}} = 0.012$ the unmirrored core transforms into the mirrored one again and starts to slip on the prism plane. For completeness, we applied basal strains ϵ_{basal} to the cores as well. The mirrored core starts to move along prismatic planes at $\epsilon_{\text{basal}} = 0.012$ and the unmirrored core again transforms into the mirrored one under $\epsilon_{\text{basal}} = 0.015$ and moves on prismatic planes. This suggests that the mirrored core is the ground state and is the dominant core configuration, even under stress. The unmirrored core is not expected to impact the mechanical behavior of Ti; it appears to be a metastable artifact of relaxing the dislocation from the initial displacements of anisotropic elasticity theory for a perfect dislocation.

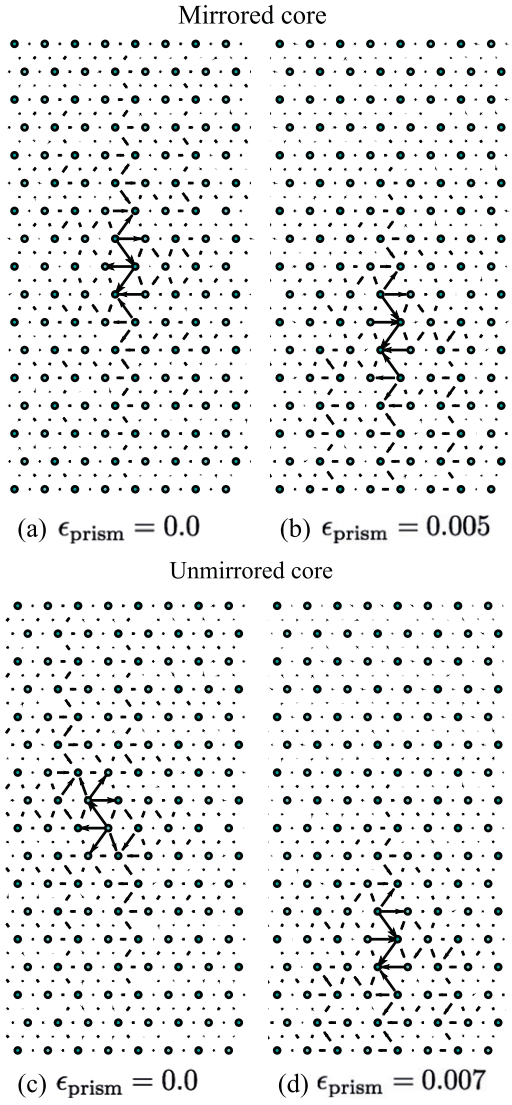

Fig. 6. Screw dislocation MEAM cores under strain on the prism plane. (a) and (c) Show mirrored and unmirrored cores under zero applied strain, respectively. The mirrored core moves under $\epsilon_{\text{prism}} = 0.005$ (b), while the unmirrored core reconstructs into the mirrored one and moves at $\epsilon_{\text{prism}} = 0.007$ (d). The unmirrored core transforms into the mirrored core under $\epsilon_{\text{pyramidal}} = 0.012$ and $\epsilon_{\text{basal}} = 0.015$ as well (not shown).

5. Conclusions

We investigated the existence of metastable core structures for a $1/3[1\bar{2}10]$ screw dislocation in Ti using DFT and MEAM potential in a framework with flexible boundary conditions. Both cores have been reproduced (in Ref. [4] and in this work) using different potentials and boundary conditions. In addition, we studied the behavior of the two cores under applied strain at $T = 0$ K and found that the higher-energy core (unmirrored) always reconstructs into the lower-energy one (mirrored) independent of the applied stain direction. We did not observe the transformation from low- to high-energy core, which rules out the possibility of transition states existing. Both dislocations continued to slip on the prism plane under sufficient strain.

This is a good extension of the results obtained in Ref. [4] and would leave open the question as to the possibility of transformation from mirrored to unmirrored core under the combination of an appropriate stress field and high temperature. We also showed that the MEAM potential agrees well with DFT in computing SFEs and dislocation core structures. Note that although the MEAM basal SFE is lower than the prismatic value, the dislocation core structures still agree closely with DFT. The agreement of MEAM and DFT is an important result suggesting that the MEAM potential is a reliable approximation for DFT in modeling dislocations in Ti and can be used in calculations that require large numbers of atoms beyond the scope of DFT.

Acknowledgments

This research was supported by NSF/CMMI Grant 0846624. Computational resources are provided by the NSF through the TeraGrid Program at TACC and in part by the Taub cluster at the University of Illinois at Urbana-Champaign.

References

[1] Hirth JP, Lothe J. Theory of dislocations. 2nd ed. New York: John Wiley & Sons; 1982.
[2] Serra A, Bacon DJ. Acta Metall Mater 1995;43:4465.
[3] Bacon D, Vitek V. Metall Mater Trans A 2002;33A:721.
[4] Tarrat N, Benoit M, Morillo J. Int J Mater Res 2009;100:329–32.
[5] Woodward C, Rao SI. Phys Rev Lett 2002;88:216402.
[6] Woodward C, Trinkle DR, Hector LG, Olmsted DL. Phys Rev Lett 2008;100:045507.
[7] Lawler HM, Trinkle DR. Phys Rev B 2010;82:172101.
[8] Yasi JA, Nogaret T, Trinkle DR, Qi Y, Hector Jr LG, Curtin WA. Modell Simul Mater Sci Eng 2009;17:055012.
[9] Hennig RG, Lenosky TJ, Trinkle DR, Rudin SP, Wilkins JW. Phys Rev B 2008;78:054121.
[10] Sinclair JE, Gehlen PC, Hoagland RG, Hirth JP. J Appl Phys 1978;49(7):3890–7.
[11] Kresse G, Hafner J. Phys Rev B 1993;47:558–61.
[12] Kresse G, Furthmuller J. Phys Rev B 1996;54:11169–86.
[13] Pedrew JP, Wang Y. Phys Rev B 1992;45:13244–9.
[14] Plimpton SJ. J Comput Phys 1995;117:1–19. <http://lammps.sandia.gov/index.html>.
[15] Woodward C. Mater Sci Eng A 2005;400–401:59–67.
[16] Vitek V, Perrin RC, Bowen DK. Philos Mag 1970;21:1049.
[17] Hartley CS, Mishin Y. Acta Mater 2005;53:1313–21.